Solid liquid equilibrium of an antifungal drug itraconazole in different neat solvents: Determination and correlation

CrossMark

Mohd Abul Kalam [a], Sultan Alshehri [a], Aws Alshamsan [b,c], Anzarul Haque [d], Faiyaz Shakeel [a,*]

[a] Department of Pharmaceutics, College of Pharmacy, King Saud University, P.O. Box 2457, Riyadh 11451, Saudi Arabia
[b] Nanomedicine Research Unit, Department of Pharmaceutics, College of Pharmacy, King Saud University, P.O. Box 2457, Riyadh 11451, Saudi Arabia
[c] King Abdullah Institute for Nanotechnology, King Saud University, Riyadh, Saudi Arabia
[d] Department of Phytochemistry and Pharmacognosy, College of Pharmacy, Prince Sattam bin Abdul Aziz University, Alkharj, Saudi Arabia

ABSTRACT

The information regarding thermodynamic parameters on solid-liquid equilibrium (SLE) of itraconazole (ITR) in different neat solvents is essential for its pharmaceutical and industrial applications. The SLE of ITR in different neat solvents had not been studied previously in literature. Hence, in this study, the SLE of ITR in various neat solvents including "water, ethanol, isopropanol (IPA), ethylene glycol (EG), propylene glycol (PG), *n*-butanol, ethyl acetate (EA), dimethyl sulfoxide (DMSO), polyethylene glycol-400 (PEG-400) and Transcutol®" was determined and correlated at temperatures "$T = 298.2$ K to 318.2 K" and pressure "$p = 0.1$ MPa". The experimental solubilities of ITR in mole fraction were determined by shake flask method and correlated with "Van't Hoff and Apelblat models". The measured solubility values of ITR in mole fraction were correlated well with "Van't Hoff and Apelblat models" with root mean square deviation values of <5.0%. The mole fraction solubility values of ITR were increasing with increase in temperature in all neat solvents investigated. The solubility of ITR was obtained highest in Transcutol (9.80×10^{-4}) followed by DMSO (8.79×10^{-4}), PEG-400 (4.62×10^{-4}), EA (3.35×10^{-4}), ethanol (4.84×10^{-5}), *n*-butanol (4.46×10^{-5}), IPA (3.58×10^{-5}), PG (2.12×10^{-5}), EG (9.85×10^{-6}) and water (8.12×10^{-8}) at $T = 318.2$ K. The solubilities of ITR were obtained in similar magnitude in Transcutol and DMSO, PEG-400 and EA and ethanol, IPA and *n*-butanol. The results of "apparent thermodynamic analysis" showed an "endothermic and entropy-driven dissolution" of ITR in each solvent evaluated.

© 2017 Elsevier B.V. All rights reserved.

1. Introduction

Itraconazole (ITR) [Fig. 1; IUPAC name: 2-butan-2-yl-4-[4-[4-[4-[[(2R,4S)-2-(2,4-dichlorophenyl)-2-(1,2,4-triazol-1-ylmethyl)-1,3-dioxolan-4-yl]methoxy]phenyl]piperazin-1-yl]phenyl]-1,2,4-triazol-3-one); molecular formula: $C_{35}H_{38}Cl_2N_8O_4$; molar mass: 705.64 g mol^{-1} and CAS number: 84625-61-6) occurs as a white to slightly yellowish crystalline powder [1,2]. It has been categorized as a broad-spectrum antifungal drug which is effective against clinical isolates of various pathogenic fungal species [1,3]. According to the biopharmaceutical classification system (BCS), it is a BCS class II drug which had high intestinal permeability and poor solubility [1,3–5]. Due to its poor solubility in water and body fluids, its oral bioavailability is very low after oral administration [3]. It is rapidly absorbed after oral administration and its bioavailability has been reported as around 55% after oral administration of ITR capsules [1,3]. Its pKa value has been reported as 3.7 and its partition coefficient in *n*-octanol/water was obtained as 5.66 at pH

of 8.1 [1]. The solid-liquid equilibrium (SLE) of poorly water-soluble compounds in various "aqueous and organic solvents" have significant importance in their preliminary studies, pharmaceutical/chemical engineering and for their industrial applications [6–11]. Therefore, it is important to determine the SLE of ITR in various aqueous and organic solvents in order to obtain its complete physicochemical information. Various formulation approaches such as solid dispersions [12–19], cyclodextrin complexation [20–22], eutectic mixture [23], mesoporous silica particles [24], nanocrystal [3], nanosphere [25], nanoemulsion [26], microemulsion [27] and noisome [28] of ITR were evaluated for the enhancement of its solubility, *in vitro* dissolution rate, drug delivery potential or *in vivo* bioavailability. The solubility data of ITR in some neat solvents including water, ethanol, isopropyl alcohol (IPA) and polyethylene glycol-400 (PEG-400) at temperature "$T = 298.2$ K" are available in literature [2,21]. However, the SLE/solubility data of ITR in neat solvents including "water, ethanol, IPA, ethylene glycol (EG), propylene glycol (PG), PEG-400, *n*-butanol, ethyl acetate (EA), Transcutol® and dimethyl sulfoxide (DMSO)" with respect to various temperatures are not reported in literature. Hence, in this study, the SLE/solubility of ITR in ten different neat solvents including "water, ethanol, Transcutol,

* Corresponding author.
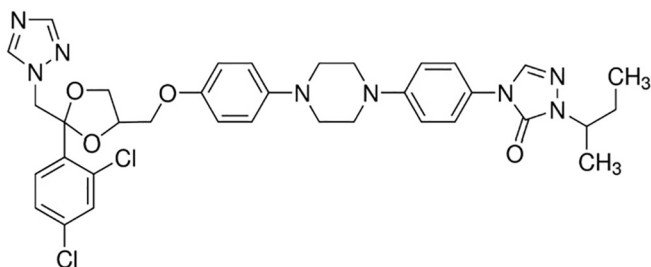*E-mail address:* faiyazs@fastmail.fm (F. Shakeel).

Fig. 1. Molecular structure of itraconazole (ITR) [molar mass: 705.64 g mol^{-1}].

PEG-400, PG, EG, IPA, *n*-butanol, EA and DMSO" were measured and correlated at "$T = 298.2$ K to 318.2 K" and pressure "$p = 0.1$ MPa". "Apparent thermodynamic analysis" on measured SLE/solubility data of ITR was also carried out by "Van't Hoff and Krug et al. analysis" in order to evaluate the dissolution behavior of ITR. The SLE/solubility data of ITR of in this research would be useful in preliminary studies, chemical/pharmaceutical engineering and industrial applications of ITR.

2. Experimental

2.1. Materials

ITR, *n*-butyl alcohol (IUPAC name: *n*-butanol) and IPA (IUPAC name: isopropanol) were obtained from "Sigma Aldrich (St. Louis, MO)". Transcutol® [IUPAC name: 2-(2-ethoxyethoxy) ethanol] was obtained from "Gattefosse (Lyon, France)". PEG-400 (IUPAC name: polyethylene glycol-400), PG (IUPAC name: 1,2-propanediol), EG (IUPAC name: 1,2-ethanediol), EA (IUPAC name: ethyl ethanoate) and DMSO (IUPAC name: dimethyl sulfoxide) were obtained from "E-Merck (Darmstadt, Germany)". Ethyl alcohol (IUPAC name: ethanol) was obtained from "Scharlab SL (Barcelona, Spain)". Water was obtained from "Milli-Q water unit". The information regarding these materials along with purity and source of these materials is presented in Table 1.

2.2. UPLC analysis of ITR

"Waters Acquity H-class ultra-performance liquid chromatography (UPLC)" system coupled with a Waters diode-array-ultra-violet detector (DAD-UV) by Aqcuity "UPLC (Waters, MA) was used for the analysis of ITR in solubility samples. The chromatographic system includes quaternary solvent manager, sample manager (Aqcuity, UPLC Waters), with injection capacity of 10 μL and a column heater. The elution of ITR was performed on "Acquity UPLC BEH™ C$_{18}$ column (2.1 × 50 mm, 1.7 μm, Waters, USA)" maintained at $T = 298.2$ K. The reported liquid chromatographic method was used for the analysis of ITR contents with slight modifications [29]. In reported method, HPLC technique was used but in this work, UPLC method was used. The mobile phase was composed of 70:30% v/v ratio of acetonitrile and water (pH of water

was maintained at 3.2 with orthophosphoric acid) which was pumped at an isocratic flow rate of 0.14 mL min^{-1}. The injection volume was 10 μL and the column oven temperature was set at $T = 296.2 \pm 2$ K and detected by UV-detector at 255 nm [29]. The 'EMPOWER software" was used to control the UPLC/UV system as well as for data acquisition and processing.

2.3. Determination of ITR solubility

The solubility of ITR in various neat solvents was determined by "shake flask method" as reported in literature [30]. "Shake flask method" is one of the commonly used methods to achieve SLE of solutes [7–9,30]. Hence, this method was applied in the current research work in order to achieve SLE of ITR. The solubility of ITR in each neat solvent was determined at "$T = 298.2$ K to 318.2 K" and "$p = 0.1$ MPa". The excess amount of ITR was added in known amounts of each solvent in triplicates manner. Each ITR-solvent mixture was vortexed for about 5 min and kept into the "Biological Shaker (Julabo, PA)" at 100 rpm for 72 h. Preliminary studies were performed to optimize SLE time for ITR. The optimum SLE time for ITR was recorded as 72 h. After SLE reach, each ITR-solvent mixture was removed from the shaker and allowed to settle ITR particles for 24 h [31]. After 24 h settling of ITR particles, the supernatants were taken, diluted suitably with mobile phase (wherever applicable) and subjected for the analysis of ITR content by the proposed UPLC technique at 255 nm described in above section. The calibration curve was plotted between the concentration of ITR and measured UPLC area. The calibration curve for ITR was obtained linear in the concentration range of (0.5 to 125.0) μg g^{-1} with coefficient of determination (R^2) value of 0.9946. The experimental solubilities of ITR (x_e) expressed as mole fraction were then calculated with the help of Eq. (1) [31,32]:

$$x_e = \frac{m_1/M_1}{m_1/M_1 + m_2/M_2} \tag{1}$$

in which, m_1 and m_2 represent the masses of ITR and respective neat solvent in g, respectively. M_1 and M_2 represent the molar masses of ITR and respective neat solvent in g mol^{-1}, respectively.

3. Results and discussion

3.1. Experimental solubility data of ITR with literature comparison

The x_e values of ITR determined by shake flask method in ten different neat solvents at "$T = 298.2$ K to 318.2 K" and "$p = 0.1$ MPa" are furnished in Table 2. The solubility data of ITR at $T = 298.2$ K in some neat solvents such as "water, ethanol, IPA and PEG-400" are available in literature [2,21]. However, the solubility data of ITR with respect to various temperatures in any of the investigated neat solvent are not available in literature so far. The mole fraction solubility of ITR in water at "$T = 298.2$ K" was obtained as 3.52×10^{-8} [21]. The

Table 1
A sample table for materials used in solubility experiment.

Compound	Molecular formula	Molar mass (g mol^{-1})	CAS registry no.	Purification method	Mass fraction purity	Analysis method	Source
ITR	C$_{35}$H$_{38}$Cl$_2$N$_8$O$_4$	705.64	84625-61-6	None	0.980	HPLC	Sigma Aldrich
Ethanol	C$_2$H$_5$OH	46.07	64-17-5	None	0.999	GC	Scharlab SL
EG	C$_2$H$_6$O$_2$	62.07	107-21-1	None	0.996	GC	E-Merck
Transcutol	C$_6$H$_{14}$O$_3$	134.17	111-90-0	None	0.999	GC	Gattefosse
PG	C$_3$H$_8$O$_2$	76.09	57-55-6	None	0.995	GC	E-Merck
PEG-400	H(OCH$_2$CH$_2$)$_n$OH	400	25322-68-3	None	0.999	HPLC	E-Merck
IPA	C$_3$H$_8$O	60.10	67-63-0	None	0.997	GC	Sigma Aldrich
n-Butanol	C$_4$H$_{10}$O	74.12	71-36-3	None	0.998	GC	Sigma Aldrich
DMSO	C$_2$H$_6$OS	78.13	67-68-5	None	0.990	GC	E-Merck
EA	C$_4$H$_8$O$_2$	88.11	141-78-6	None	0.997	GC	E-Merck
Water	H$_2$O	18.07	7732-18-5	None	–	–	Milli-Q

Both the analysis method and mass fraction purity were provided by supplier.

Table 2

Measured solubilities (x_e) of ITR in mole fraction in ten different neat solvents (S) at "$T = 298.2$ K to 318.2 K" and "$p = 0.1$ MPa".[a]

S	x_e				
	$T = 298.2$ K	$T = 303.2$ K	$T = 308.2$ K	$T = 313.2$ K	$T = 318.2$ K
Water	1.44×10^{-8}	2.48×10^{-8}	3.86×10^{-8}	5.80×10^{-8}	8.12×10^{-8}
Ethanol	1.58×10^{-5}	2.23×10^{-5}	2.94×10^{-5}	3.92×10^{-5}	4.84×10^{-5}
IPA	1.64×10^{-5}	1.96×10^{-5}	2.38×10^{-5}	2.88×10^{-5}	3.58×10^{-5}
EG	5.08×10^{-6}	6.07×10^{-6}	7.13×10^{-6}	8.46×10^{-6}	9.85×10^{-6}
PG	9.06×10^{-6}	1.10×10^{-5}	1.36×10^{-5}	1.68×10^{-5}	2.12×10^{-5}
PEG-400	2.47×10^{-4}	2.98×10^{-4}	3.50×10^{-4}	4.02×10^{-4}	4.62×10^{-4}
Transcutol	4.27×10^{-4}	5.42×10^{-4}	6.87×10^{-4}	8.36×10^{-4}	9.80×10^{-4}
n-Butanol	2.09×10^{-5}	2.60×10^{-5}	3.12×10^{-5}	3.59×10^{-5}	4.46×10^{-5}
EA	2.09×10^{-4}	2.35×10^{-4}	2.68×10^{-4}	3.02×10^{-4}	3.35×10^{-4}
DMSO	3.81×10^{-4}	4.94×10^{-4}	6.16×10^{-4}	7.39×10^{-4}	8.79×10^{-4}

[a] The standard uncertainties u are $u(T) = 0.10$ K, $u(p) = 0.003$ MPa and $u_r(x_e) = 1.54\%$.

mole fraction solubility of ITR in water at "$T = 298.2$ K" was obtained as 1.44×10^{-8} in the current research work. The solubility of ITR as mole fraction in ethanol, IPA and PEG-400 at $T = 298.2$ K have been reported as 1.96×10^{-5}, 6.43×10^{-6} and 2.22×10^{-4}, respectively [2]. The solubility of ITR as mole fraction in ethanol, IPA and PEG-400 at $T = 298.2$ K were obtained as 1.58×10^{-5}, 1.64×10^{-5} and 2.48×10^{-4}, respectively in this work. The mole fraction solubility of ITR in water, ethanol and PEG-400 obtained in this work was very close to that reported in literature. However, the solubility of ITR in IPA was slightly deviated from its reported value. This deviation could be due to little change in SLE time and speed of shaker.

Generally, the x_e values of ITR in the current research work were observed as increasing with increase in temperature in all neat solvents evaluated (Table 2). The x_e values of ITR were obtained highest in Transcutol (9.80×10^{-4}) followed by DMSO (8.79×10^{-4}), PEG-400 (4.62×10^{-4}), EA (3.35×10^{-4}), ethanol (4.84×10^{-5}), n-butanol (4.46×10^{-5}), IPA (3.58×10^{-5}), PG (2.12×10^{-5}), EG (9.85×10^{-6}) and water (8.12×10^{-8}) at $T = 318.2$ K. The x_e values of ITR were obtained in similar magnitude in Transcutol and DMSO, PEG-400 and EA and ethanol, IPA and n-butanol. The x_e values of ITR in Transcutol, DMSO, PEG-400 and EA were significantly higher than its x_e values in "water, ethanol, IPA, n-butanol, EG and water". This observation was obtained due to the fact that ITR is having several nonpolar groups and rings (Fig. 1) that would results in strong molecular interaction with nonpolar solvents such as Transcutol, DMSO, PEG-400 and EA. The highest x_e values of ITR in Transcutol were possibly due low dielectric constant/polarity of Transcutol as compared to high dielectric constant/polarity of water [31,32]. The x_e values of ITR in ethanol, IPA and n-butanol were not significantly different because all these solvents have similar dielectric constants/polarities [32]. The x_e values of ITR in PG and EG were also obtained in similar magnitude because both of the neat solvents have two —OH groups with similar dielectric constants/polarities [31].

3.2. Correlation of x_e values of ITR with mathematical models

Apelblat and Van't Hoff models are the commonly used computational models for the solubility prediction of solutes in various neat solvents [31–35]. Therefore, the x_e values of ITR were correlated and fitted with two different computational models including "Apelblat and van't Hoff models" [33–35]. The "Apelblat model solubility (x^{Apl})" of ITR was determined using Eq. (2) [33,34]:

$$\ln x^{Apl} = A + \frac{B}{T} + C \ln(T) \tag{2}$$

in which, the symbols A, B and C are the model parameters of "Apelblat model". The values of these parameters were calculated by
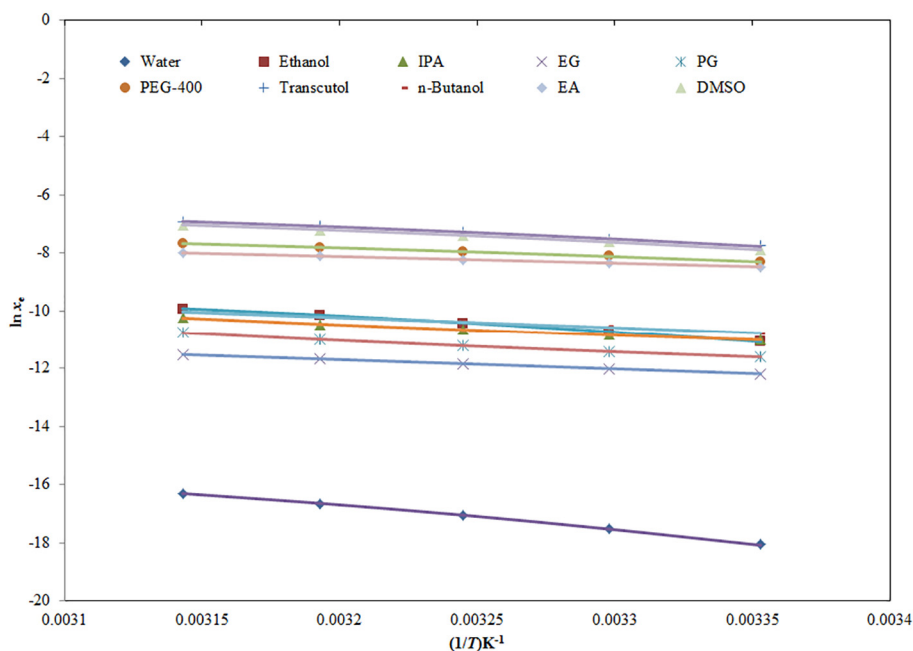

Fig. 2. Correlation/curve fitting of $\ln x_e$ values of ITR with "Apelblat model" in ten different neat solvents as a function of $1/T$; symbols represent the experimental solubilities of ITR and solid lines represent the solubilities of ITR calculated by "Apelblat model".

Table 3
The resulting data of Apelblat correlation in terms of model parameters (A, B and C), R^2 and % $RMSD$ values for ITR in ten different neat solvents (S).

S	A	B	C	R^2	$RMSD$ (%)
Water	1495.03	−76,386.20	−220.60	0.9999	2.29
Ethanol	888.48	−45,809.50	−130.91	0.9998	1.70
PG	−537.36	20,700.67	80.09	0.9999	0.62
PEG-400	355.26	−19,182.90	−52.52	0.9995	0.69
Transcutol	635.69	−32,911.40	−93.56	0.9992	1.15
EG	40.55	−5088.70	−6.26	0.9998	0.68
IPA	−509.85	19,770.63	75.91	0.9999	0.83
n-Butanol	−20.78	−2503.46	3.23	0.9954	1.82
EA	65.48	−5323.86	−9.84	0.9992	0.49
DMSO	695.15	−35,618.90	−102.42	0.9993	1.16

"multivariate regression analysis" of x_e values of ITR furnished in Table 2 [32]. The x_e values of ITR were fitted/correlated with its x^{Apl} values in terms of "root mean square deviations ($RMSD$)" and R^2 values. The $RMSD$ values between x_e and x^{Apl} of ITR were calculated using its standard formula reported in literature [10].

The graphical correlation/curve fitting between x_e and x^{Apl} values of ITR in ten different neat solvents against $1/T$ is shown in Fig. 2. Fig. 2 showed good graphical correlation/curve fitting between x_e and x^{Apl} values of ITR. The results of Apelblat correlation/fitting are furnished in Table 3. The values of model parameters (A, B and C) for this model were not significant ($P > 0.05$) in most of the neat solvents investigated. Therefore, the results were not correlated with model parameters. The $RMSD$ values in ten different neat solvents were recorded in the range of (0.49 to 2.29) %. The $RMSD$ value for ITR was obtained highest for neat water (2.29%) followed by *n*-butanol (1.82%), ethanol (1.70%), DMSO (1.16%), Transcutol (1.15%), IPA (0.83%), PEG-400 (0.69%), EG (0.68%), PG (0.62%) and EA (0.49%). The R^2 values for ITR in ten different neat solvents were recorded in the range of 0.9954 to 0.9999. The lower values of $RMSD$ and higher values of R^2 for ITR showed good correlation of x_e values of ITR with "Apelblat model".

The "Van't Hoff model solubility ($x^{Van't}$)" of ITR was determined using Eq. (3) [35]:

$$\ln x^{Van't} = a + \frac{b}{T} \tag{3}$$

in which, the symbols "a and b" are the model parameters of "Van't Hoff model". The values of these parameters were calculated by plotting $\ln x_e$ values of ITR against $1/T$.

The x_e values of ITR were correlated/fitted with $x^{Van't}$ values with the help of $RMSD$ and R^2 values [32].

The graphical correlation/curve fitting between x_e and $x^{Van't}$ values of ITR in ten different neat solvents against $1/T$ is shown in Fig. 3. Fig. 3 presented good correlation/curve fitting. The results of Van't Hoff correlation are furnished in Table 4. The values of model parameters (a, and b) for this model were not significant ($P > 0.05$) in most of the neat solvents investigated. Therefore, the results were not correlated with model parameters. The $RMSD$ values for ITR in ten different neat solvents were recorded in the range of (0.31 to 4.27) %. The $RMSD$ value for ITR was also obtained highest for neat water (4.27%) followed by ethanol (2.48%), DMSO (2.01%), Transcutol (1.90%), *n*-butanol (1.75%), PG (1.50%), IPA (1.45%), PEG-400 (1.05%), EA (0.47%) and EG (0.31%). The R^2 values for ITR in ten different neat solvents were recorded in the range of 0.9953 to 0.9998. The lower values of $RMSD$ and higher values of R^2 for ITR again showed good correlation of x_e values of ITR with "Van't Hoff model".

3.3. Apparent thermodynamic analysis

"Apparent thermodynamic analysis" of SLE/solubility data of ITR was performed for the evaluation of the dissolution behavior of ITR in ten
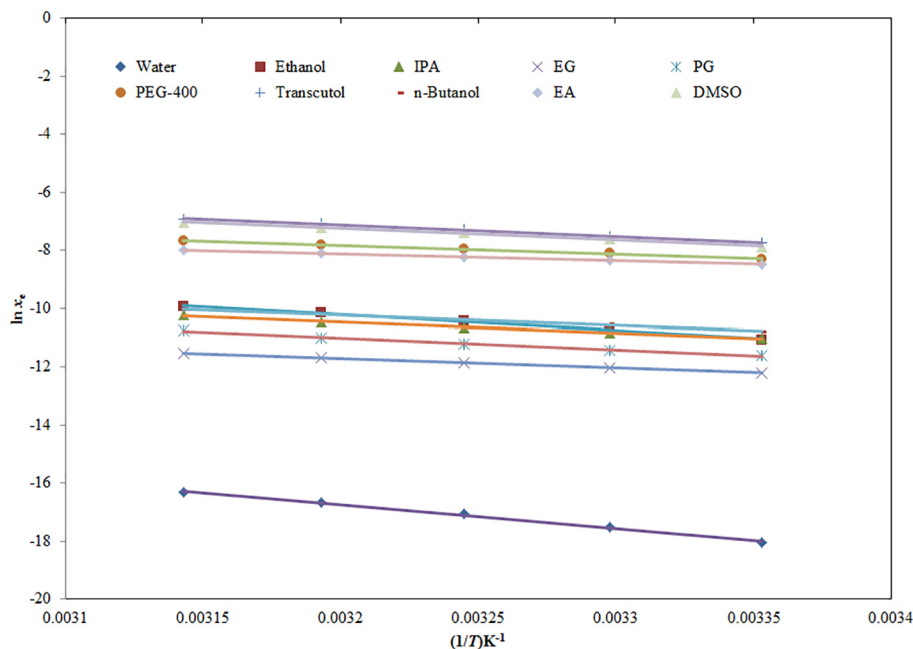

Fig. 3. Correlation/curve fitting of experimental natural logarithmic solubilities ($\ln x_e$) of ITR with Van't Hoff model in different mono solvents as a function of $1/T$; symbols represent the experimental $\ln x_e$ values of ITR and the solid lines represent the $\ln x^{Van't}$ values calculated by Van't Hoff model.

Table 4
The resulting data of Van't Hoff model in terms of model parameters (a and b), R^2 and % $RMSD$ values for ITR in ten different neat solvents (S).

S	a	b	R^2	$RMSD$ (%)
Water	9.41	−8176.80	0.9955	4.27
Ethanol	6.84	−5329.00	0.9961	2.48
PG	1.91	−4038.10	0.9973	1.50
PEG-400	1.57	−2940.60	0.9977	1.05
Transcutol	5.60	−3980.40	0.9959	1.90
EG	−1.65	−3142.10	0.9998	0.31
IPA	1.30	−3678.40	0.9971	1.45
n-Butanol	0.93	−3490.10	0.9955	1.75
EA	−0.85	−2272.30	0.9991	0.47
DMSO	5.39	−3949.50	0.9953	2.01

different neat solvents. Therefore, different "apparent standard thermodynamic parameters" including "apparent standard dissolution enthalpy ($\Delta_{sol}H^0$), apparent standard Gibbs free energy ($\Delta_{sol}G^0$) and apparent standard dissolution entropy ($\Delta_{sol}S^0$)" of ITR dissolution were measured. The "$\Delta_{sol}H^0$ values" for ITR dissolution in ten different neat solvents were measured at "mean harmonic temperature (T_{hm})" value of 308 K by applying Van't Hoff analysis using Eq. (4) [36,37]:

$$\left(\frac{\partial \ln x_e}{\partial \left(1/T - 1/T_{hm} \right)} \right)_P = -\frac{\Delta_{sol}H^0}{R} \tag{4}$$

The "$\Delta_{sol}H^0$ values" for ITR dissolution were calculated by plotting ln x_e values of ITR against $1/T - 1/T_{hm}$. The results of Van't Hoff analysis are presented in Fig. 4. These Van't Hoff plots for ITR dissolution in ten different neat solvents were obtained as linear with R^2 values of 0.9952 to 0.9999 (Fig. 4).

The "$\Delta_{sol}G^0$ values" for ITR dissolution were also measured at T_{hm} value of 308 K by applying the approach of "Krug et al. analysis" using Eq. (5) [38]:

$$\Delta_{sol}G^0 = -RT_{hm} \times \text{intercept} \tag{5}$$

in which, the value of intercept for ITR in each neat solvent was determined from "Van't Hoff plot" constructed between ln x_e values of ITR and $1/T - 1/T_{hm}$.

Finally, the "$\Delta_{sol}S^0$ values" for ITR dissolution were measured by applying the combined approach of "Van't Hoff and Krug et al. analysis" using Eq. (6) [36–38]:

$$\Delta_{sol}S^0 = \frac{\Delta_{sol}H^0 - \Delta_{sol}G^0}{T_{hm}} \tag{6}$$

The resulting data of "apparent thermodynamic analysis" along with R^2 values for ITR dissolution in ten different neat solvents are furnished in Table 5.

From "apparent thermodynamic analysis", it was observed that the "$\Delta_{sol}H^0$ values" for ITR dissolution in all solvents were obtained as positive values in the range of (23.07 to 68.07) kJ mol^{-1}. The "$\Delta_{sol}H^0$ value" for ITR dissolution was obtained highest in water (68.07 kJ mol^{-1}) followed by ethanol (44.36 kJ mol^{-1}), EG (37.28 kJ mol^{-1}), PG (33.62 kJ mol^{-1}), Transcutol (33.13 kJ mol^{-1}), DMSO (32.87 kJ mol^{-1}), IPA (30.62 kJ mol^{-1}), n-butanol (29.05 kJ mol^{-1}), PEG-400 (24.47 kJ mol^{-1}) and EA (23.07 kJ mol^{-1}). The mean "$\Delta_{sol}H^0$ value" for ITR dissolution was recorded as 35.65 kJ mol^{-1} with relative standard deviation (RSD) value of 0.36. The highest "$\Delta_{sol}H^0$ value" for ITR dissolution was obtained in water that was possible due to the lowest solubility of ITR in water. Generally, the "$\Delta_{sol}H^0$ values" were higher for ITR dissolution in all neat solvents investigated which indicated that some extent of energy is required for the solubilization of ITR in these solvents. The "$\Delta_{sol}G^0$ values" for ITR dissolution in all solvents were also obtained as positive
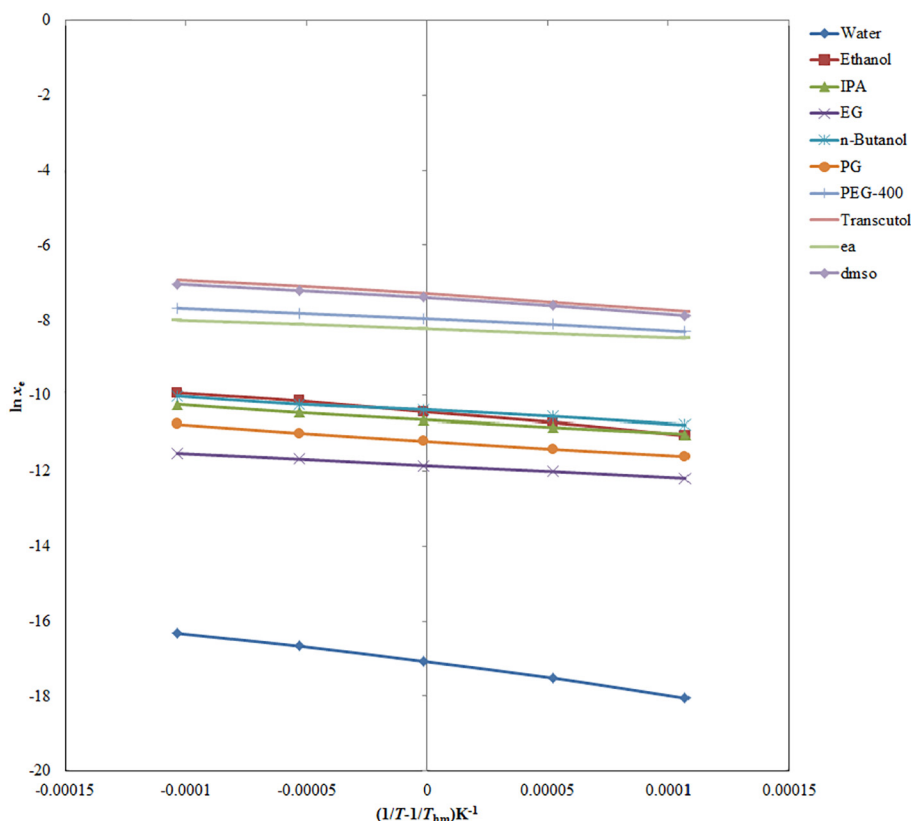

Fig. 4. Van't Hoff plots for ITR between ln x_e and $1/T$-$1/T_{hm}$ in ten different mono solvents.

Table 5
The results of "Apparent thermodynamic analysis" in terms of various thermodynamic quantities and R^2 values for ITR dissolution in ten different neat solvents.[b]

Parameters	Water	Ethanol	PG	PEG-400	Transcutol	EG	IPA	n-Butanol	EA	DMSO
$\Delta_{sol}H^0$/kJ mol^{-1}	68.07	44.36	33.62	24.47	33.13	37.28	30.62	29.05	23.07	32.87
$\Delta_{sol}G^0$/kJ mol^{-1}	43.85	26.77	28.67	20.42	18.73	30.38	27.24	26.60	21.08	19.01
$\Delta_{sol}S^0$/J mol^{-1} K^{-1}	78.61	57.09	16.05	13.17	46.76	22.40	10.97	7.94	6.46	45.01
R^2	0.9953	0.9995	0.9975	0.9976	0.9999	0.9998	0.9972	0.9975	0.9979	0.9952

[b] The relative uncertainties are $u(\Delta_{sol}H^0) = 0.36$ kJ mol^{-1}, $u(\Delta_{sol}G^0) = 0.28$ kJ mol^{-1} and $u(\Delta_{sol}S^0) = 0.81$ J mol^{-1} K^{-1}.

values in the range of (19.01 to 43.85) kJ mol^{-1}. The "$\Delta_{sol}G^0$ value" for ITR dissolution was also obtained highest in water (43.85 kJ mol^{-1}) followed by EG (30.38 kJ mol^{-1}), PG (28.67 kJ mol^{-1}), IPA (27.24 kJ mol^{-1}), ethanol (26.77 kJ mol^{-1}), n-butanol (26.60 kJ mol^{-1}), EA (21.08 kJ mol^{-1}), PEG-400 (20.42 kJ mol^{-1}), DMSO (19.01 kJ mol^{-1}) and Transcutol (18.13 kJ mol^{-1}). The mean "$\Delta_{sol}G^0$ value" for ITR dissolution was recorded as 26.27 kJ mol^{-1} with RSD value of 0.28. The highest "$\Delta_{sol}G^0$ value" for ITR dissolution was also obtained in water that was possible due to the lowest solubility of ITR in water. Generally, the "$\Delta_{sol}G^0$ values" were also higher for ITR dissolution in all neat solvents investigated which indicated that some extent of energy is required for the solubilization of ITR in these solvents. The results of $\Delta_{sol}G^0$ values for ITR dissolution were in good agreement with measured solubility data of ITR. The positive values of "$\Delta_{sol}H^0$ and $\Delta_{sol}G^{0}$" in all neat solvents showed an "endothermic dissolution" behavior of ITR in all neat solvents evaluated [39]. The "$\Delta_{sol}S^0$ values" for ITR dissolution were also obtained as positive values in the range of (6.46 to 78.61) J mol^{-1} K^{-1} in all neat solvents evaluated (Table 5). The mean "$\Delta_{sol}S^0$ value" for ITR dissolution was recorded as 30.44 J mol^{-1} K^{-1} with RSD value of 0.81. The positive "$\Delta_{sol}S^0$ values" showed an "entropy-driven dissolution' of ITR in all neat solvents evaluated [40]. Overall, the dissolution behavior of ITR was recorded as an "endothermic and entropy-driven" in all neat solvents evaluated [39,40].

4. Conclusion

The SLE of an antifungal drug ITR was determined in ten different neat solvents at "$T = 298.2$ K to 318.2 K" and "$p = 0.1$ MPa". The solubility of ITR in mole fraction was determined by "shake flask method" and correlated with "Van't Hoff and Apelblat" models. The RMSD values for ITR were obtained as <5.0% for both models, indicating good correlation of experimental solubility data of ITR with both of the models. The solubility of ITR was observed as increasing with increase in temperature in all solvents evaluated. The solubility of ITR in mole fraction was obtained highest Transcutol (9.80×10^{-4}) followed by DMSO, PEG-400, EA, ethanol, n-butanol, IPA, PG, EG and water at $T = 318.2$ K. "Apparent thermodynamic analysis" of solubility data of ITR showed an "endothermic and entropy-driven dissolution" of ITR in all solvents evaluated.

Conflict of interest

The authors report no conflict of interest associated with this manuscript.

List of symbols

x_e	experimental mole fraction solubilities
x^{Apl}	mole fraction solubilities calculated by Apelblat model
$x^{Van't}$	mole fraction solubilities calculated by Van't Hoff model
m_1	mass of solute
m_2	mass of solvent
M_1	molar mass of solute
M_2	molar mass of solvent
T	absolute temperature
p	atmospheric pressure
T_{hm}	mean harmonic temperature
A, B, C	model parameters of Apelblat model
a, b	model parameters of Van't Hoff model
RMSD	root mean square deviations
RSD	relative standard deviations
R	universal gas constant
R^2	coefficient of determination
T	absolute temperature
$\Delta_{sol}H^0$	apparent standard enthalpy
$\Delta_{sol}G^0$	apparent standard Gibbs free energy
$\Delta_{sol}S^0$	apparent standard entropy

References

[1] J.P. Pawar, T.M. Ali, K.K. Moravkar, R.K. Patole, D.S. Jaiswar, P.D. Amin, Recent development and achievement in solubility and dissolution enhancement of itraconazole: a review, Int. J. Pharm. Sci. Res. 5 (2014) 3096–3106.
[2] P. Sriamornsak, K. Burapapadh, Characterization of recrystallized itraconazole prepared by cooling and anti-solvent crystallization, Asian J. Pharm. Sci. 10 (2015) 230–238.
[3] L. De Smet, L. Saerens, T. De Beer, R. Carleer, P. Adriaensens, J.V. Bocxlaer, C. Vervaet, J.P. Remon, Formulation of itraconazole nanococrystals and evaluation of their bioavailability in dogs, Eur. J. Pharm. Biopharm. 87 (2014) 107–113.
[4] E. Merisko-Liversidge, G.G. Liversidge, Nanosizing for oral and parenteral drug delivery: a perspective on formulating poorly-water soluble compounds using wet media milling technology, Adv. Drug Deliv. Rev. 63 (2011) 427–440.
[5] B. Van Eerdenbrugh, G. Van den Mooter, P. Augustijns, Top-down production of drug nanocrystals: nanosuspension stabilization, miniaturization and transformation into solid products, Int. J. Pharm. 364 (2008) 64–75.
[6] M.K. Anwer, R. Al-Shdefat, S. Jamil, P. Alam, M.S. Abdel-Kader, F. Shakeel, Solubility of bioactive compound hesperidin in six pure solvents at (298.15 to 333.15) K, J. Chem. Eng. Data 59 (2014) 2065–2069.
[7] F. Shakeel, N. Haq, N.A. Siddiqui, Solubility and thermodynamic function of vanillin in ten different environmentally benign solvents, Food Chem. 180 (2015) 244–248.
[8] F. Shakeel, N. Haq, N.A. Siddiqui, F.K. Alanazi, I.A. Alsarra, Solubility and thermodynamic behavior of vanillin in propane-1,2-diol + water cosolvent mixtures at different temperatures, Food Chem. 188 (2015) 57–61.
[9] F. Shakeel, N. Haq, N.A. Siddiqui, F.K. Alanazi, I.A. Alsarra, Solubility and thermodynamics of vanillin in Carbitol-water mixtures at different temperatures, LWT Food Sci. Technol. 64 (2015) 1278–1282.
[10] G. Wu, Y. Hu, P. Gu, W. Yang, C. Wang, Z. Ding, R. Deng, T. Li, H. Hong, Determination and correlation thermodynamic models for solid–liquid equilibrium of the nifedipine in pure and mixture organic solvents, J. Chem. Thermodyn. 102 (2016) 333–340.
[11] Y. Yu, T. Li, Y. Hu, W. Yang, Y. Zhang, R. Deng, M. Jiang, Equilibrium study and diversified models of drug norfloxacin in eight pure organic and binary solvents at T = (278.15–328.15) K, Fluid Phase Equilib. 435 (2017) 45–59.
[12] J.Y. Jung, S.D. Yoob, S.H. Lee, K.H. Kim, D.S. Yoon, K.H. Lee, Enhanced solubility and dissolution rate of itraconazole by a solid dispersion technique, Int. J. Pharm. 187 (1999) 209–218.
[13] K.P.R. Chowdary, S.K.S. Rao, Investigation of dissolution enhancement of itraconazole by solid dispersion in superdisintegrants, Drug Dev. Ind. Pharm. 26 (2000) 1207–1211.
[14] G.M. El-Maghraby, A.H. Alomrani, Synergistic enhancement of itraconazole dissolution by ternary system formulation with Pluronic F68 and hydroxypropylmethylcellulose, Sci. Pharm. 77 (2009) 401–417.
[15] R.S. Prasad, S.K. Yandrapu, R. Manavalan, Preparation and characterization of itraconazole solid dispersions for improved oral bioavailability, Int. J. Chem. Tech. Res. 12 (2010) 133–142.
[16] A.K. Garg, R.K. Sachdeva, G. Kapoor, Comparison of crystalline and amorphous carriers to improve the dissolution profile of water insoluble drug itraconazole, Int J Pharm. Bio. Sci 4 (2013) 934–948.
[17] B. Lang, J.W. McGinity, R.O. WilliamsIII, Dissolution enhancement of itraconazole by holt-melt extrusion alone and the combination of holt-melt extrusion and rapid

freezing-effect of formulation and processing variable, Mol. Pharm. 11 (2014) 186–196.

[18] M.K. Kataria, A. Bhandari, Solubility and dissolution rate enhancement of itraconazole by solid dispersion technique, Indo. Amer. J. Pharm. Res. 4 (2014) 849–863.

[19] T. Parikh, H.K. Sandhu, T.T. Talele, A.T.M. Sirajuddin, Characterization of solid dispersion of itraconazole prepared by solibilization in concentrated aqueous solutions of weak organic acids and drying, Pharm. Res. 33 (2016) 1456–1471.

[20] L. Srinivas, V.S.V.K. Tenneti, B.N.M. Rao, B.B. Teja, Preparation and evaluation of itraconazole cyclodextrin complexes to enhance their solubility and dissolution parameters, Amer. J. Pharm. Res. 4 (2014) 827–847.

[21] H. Bagavatula, S. Lankalapalli, V.S.V.K. Teneneti, N.M.R. Beeraka, B.T. Bulusu, Comparative studies on solubility and dissolution enhancement of different itraconazole salts and their complexes, Adv. Pharmacol. Pharm. 2 (2014) 85–95.

[22] L. Srinivas, B. Hemalatha, V.S.V.K. Tenneti, N.M.R. Beeraka, B.T. Bulusu, Studies on solubility and dissolution enhancement of itraconazole by complexation with sulfo-butyl7 ether β cyclodextrin, Asian J. Biomed. Pharm. Sci. 4 (2014) 6–16.

[23] D. Liu, X. Fie, S. Wang, T. Jiang, D. Su, Increasing solubility and dissolution rate of drugs via eutectic mixtures: itraconazole-poloxamer 188 system, Asian J. Pharm. Sci. 1 (2006) 213–221.

[24] X. Liu, S. Che, Enhanced release of poorly soluble drug itraconazole loaded in ordered mesoporous silica, SCIENCE CHINA Chem. 58 (2015) 400–410.

[25] X. Bian, S. Liang, J. John, C.H. Hsiao, X. Wei, D. Liang, H. Xie, Development of PLGA-based itraconazole injectable nanospheres for sustained release, Int. J. Nanomedicine 8 (2013) 4521–4531.

[26] H.P. Thakkar, A. Khunt, R.D. Dhande, A.A. Patel, Formulation and evaluation of itraconazole nanoemulsion for enhanced oral bioavailability, J. Microencapsul. 32 (2015) 559–569.

[27] N. Kumar, Shishu, D-optimal experimental approach for designing topical microemulsion of itraconazole: characterization and evaluation of antifungal efficacy against a standardized Tinea pedis infection model in Wistar rats, Eur. J. Pharm. Sci. 67 (2015) 97–112.

[28] N. Kumar, S. Goindi, Statistically designed nonionic surfactant vesicles for dermal delivery of itraconazole: characterization and in vivo evaluation using a standardized Tinea pedis infection model, Int. J. Pharm. 472 (2014) 224–240.

[29] G.A. Khoschsorur, F. Fruehwirth, S. Zelzer, Isocratic high-performance liquid chromatographic method with ultraviolet detection for simultaneous determination of levels of voriconazole and itraconazole and its hydroxy metabolite in human serum, Antimicrob. Agents Chemother. 49 (2005) 3569–3571.

[30] T. Higuchi, K.A. Connors, Phase-solubility techniques, Adv. Anal. Chem. Instrum. 4 (1965) 117–122.

[31] F. Almarri, N. Haq, F.K. Alanazi, K. Mohsin, I.A. Alsarra, F.S. Aleanizy, F. Shakeel, Solubility and thermodynamic function of vitamin D3 in different mono solvents, J. Mol. Liq. 229 (2017) 477–481.

[32] F. Shakeel, M. Imran, Abida, N. Haq, F.K. Alanazi, I.A. Alsarra, Solubility and thermodynamic/solvation behavior of 6-phenyl-4,5-dihydropyridazin-3(2H)-one in different (Transcutol + water) mixtures, J. Mol. Liq. 230 (2017) 511–517.

[33] A. Apelblat, E. Manzurola, Solubilities of o-acetylsalicylic, 4-aminosalicylic, 3,5-dinitrosalicylic and p-toluic acid and magnesium-DL-aspartate in water from T = (278–348) K, J. Chem. Thermodyn. 31 (1999) 85–91.

[34] E. Manzurola, A. Apelblat, Solubilities of L-glutamic acid, 3-nitrobenzoic acid, acetylsalicylic, p-toluic acid, calcium-L-lactate, calcium gluconate, magnesium-DL-aspartate, and magnesium-L-lactate in water, J. Chem. Thermodyn. 34 (2002) 1127–1136.

[35] F. Shakeel, N. Haq, F.K. Alanazi, I.A. Alsarra, Solubility of anti-inflammatory drug lornoxicam in ten different neat solvents at different temperatures, J. Mol. Liq. 209 (2015) 280–283.

[36] A.R. Holguín, G.A. Rodríguez, D.M. Cristancho, D.R. Delgado, F. Martínez, Solution thermodynamics of indomethacin in propylene glycol + water mixtures, Fluid Phase Equilib. 314 (2012) 134–139.

[37] M.A. Ruidiaz, D.R. Delgado, F. Martínez, Y. Marcus, Solubility and preferential solvation of indomethacin in 1,4-dioxane + water solvent mixtures, Fluid Phase Equilib. 299 (2010) 259–265.

[38] R.R. Krug, W.G. Hunter, R.A. Grieger, Enthalpy-entropy compensation. 2. Separation of the chemical from the statistic effect, J. Phys. Chem. 80 (1976) 2341–2351.

[39] F. Shakeel, F.K. Alanazi, I.A. Alsarra, N. Haq, Solubility of antipsychotic drug risperidone in Transcutol + water co-solvent mixtures at 298.15 to 333.15 K, J. Mol. Liq. 191 (2014) 68–72.

[40] F. Shakeel, N. Haq, A.A. Radwan, F.K. Alanazi, I.A. Alsarra, Solubility and thermodynamic analysis of N′-(1-(N-(methyl) benzylaminomethyl)-2-oxoindolin-3-ylidene)-2-(benzyloxy) benzohydrazide in different neat solvents at different temperatures, J. Mol. Liq. 220 (2016) 108–112.